CIENCIA EN REVOLUCIÓN

Grima et al, Vol. 7, Nro. 20, 9–15, enero–abril, 2021.

Article:

Cu_3TaTe_4: Synthesis, X-ray Diffraction, Scanning Electron Microscopy, and Diffuse Reflectance Measurements

P. Grima-Gallardo[1,2,3]*, L. Nieves[1,2,3], A. Velasquez[1,2], G.E. Delgado[4]

[1]Centro Nacional de Tecnologías Ópticas, Mérida, Venezuela

[2]Centro de Investigaciones de Astronomía, Mérida, Venezuela

[3]Centro de Estudios en Semiconductores, Departamento de Física, Facultad de Ciencias Universidad de Los Andes, Mérida, Venezuela

[4]Laboratorio de Cristalografía, Departamento de Química, Facultad de Ciencias Universidad de Los Andes, Mérida, Venezuela

Recibido: marzo 2021
Aceptado: abril 2021
Autor para correspondencia: P. Grima-G. e–mail: peg1952@gmail.com
DOI: https://doi.org/10.5281/zenodo.4968549

Abstract

In the present investigation Polycrystalline samples of Cu_3TaTe_4 were prepared by the melt and anneal method. X-Ray Diffraction (*XRD*) and Diffuse Reflectance Spectroscopy (DRS) measurements were performed to verify the crystal structure and calculate the indirect and direct band gaps. The results showed a lattice parameter $a = 5.9082$ Å, a stoichiometry with a Ta deficit of 17.8 %, indirect bandgap $E_g^i = 0.38$ eV, and a direct gap $E_g^d = 2.38$ eV. The analyzes confirm that Cu_3TaTe_4 can be used as an *p*-type absorbent for thin film solar cells with the advantages that its elements have low toxicity and have lower costs than those used today.

Key words: Cu_3TaTe_4; diffuse reflectance; optical bandgap.

Artículo:

Cu_3TaTe_4: Medidas de síntesis, difracción de rayos X, microscopía electrónica de barrido y reflectancia difusa

Resumen

En la presente investigación fueron preparadas muestras policristalinas de Cu_3TaTe_4 por el método de fusión y recocido. Se realizaron medidas de difracción de rayos X (DRX) y espectroscopía de reflectancia difusa (*ERD*) para verificar la estructura cristalina y calcular las brechas de energía directa e indirecta. Los resultados mostraron un parámetro de red $a = 5,9082$ Å, una estequiometría deficitaria en Ta del 17,8 %, una brecha de energía indirecta $E_g^i = 0,38$ eV y una brecha de energía directa $E_g^d = 2,38$ eV. Los análisis confirman que el Cu_3TaTe_4 puede ser empleado como absorbente *p*-tipo para células solares de películas finas con las ventajas de que sus elementos presentan baja toxicidad y tienen costos menores a los empleados en la actualidad.

Palabras claves: Cu_3TaTe_4; reflectancia difusa; brecha óptica de energía.

1 Introduction

The sulvanite family of compounds, with chemical formula Cu_3-TM-VI_4, (TM is the transition metal V, Nb, or Ta and VI is S, Se, or Te), is composed of nine members; three sulfides: Cu_3VS_4, Cu_3NbS_4, Cu_3TaS_4; three selenides: Cu_3VSe_4, Cu_3NbSe_4, Cu_3TaSe_4; and three tellurides: Cu_3VTe_4, Cu_3NbTe_4, Cu_3TaTe_4. They are all semiconductors. As-growth samples show *p*-type electrical conductivity, high ionic mobility, low hole effective mass, high optical absorption in the visible and UV range, and optical bandgaps suitable for their use as an absorber layer in thin-film solar photovoltaic devices [1, 2].

Sulvanites crystallize in the cubic structure, space group (N 215), consisting of Cu, TM and VI atoms located at the atom-sites (Wyckoff coordinates): 3d $(0.5, 0, 0)$, 1a $(0, 0, 0)$ and 4e (u, u, u), respectively (Figure 1) [3, 4, 5], described for the first time by Pauling and Hultgren [6] for the natural mineral, Cu_3VS_4.

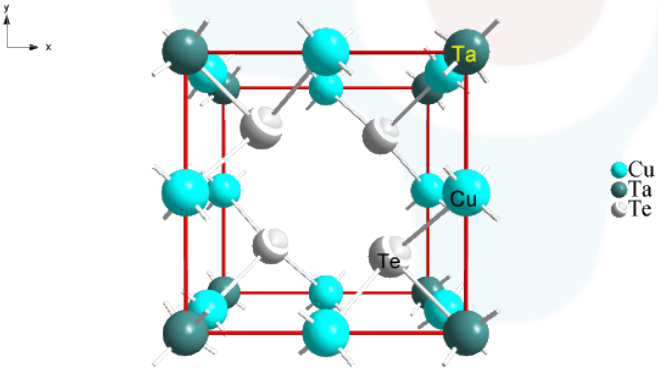

Figure 1: The unit cell of sulvanite Cu_3TaTe_4. Image created using Diamond software version 3.2e with lattice parameter $a = 6.025$ Å [7] and anion displacement $u = 0.2558$ [7]

Although this semiconductor family has been extensively studied by *ab initio* calculations [2]-[5], [7]-[17] experimental results are relatively scarce, in particular for Cu_3TaTe_4. The experimental value of the lattice parameter a for Cu_3TaTe_4 has been reported by Hulliger [18], Zitter *et al.* [19], and Li *et al.* [20] as 5.928 Å, 5.9283 Å, and 5.930(2) Å, respectively; in good agreement with theoretical calculations of Hong *et al.* (6.01 Å) [13] and Kehoe *et al.* (5.906 Å) [2], (6.033 Å) [9]. No experimental data for optical properties, as the bandgap (E_g), were found in the literature.

In this work, the measurement of the bandgap value for Cu_3TaTe_4 is reported for the first time. The bandgap is essential for applications in optoelectronic devices as light detectors and solar cells.

2 Experimental procedure

2.1 Synthesis

Polycrystalline samples of Cu_3TaTe_4 have been produced by the melt and anneal method as is described below. Starting materials (Cu, Ta, and Te) with nominal purity of 99.99 wt. % in the stoichiometric ratio were mixed in an evacuated (10^{-4} Torr) and sealed the quartz tube with the inner walls previously carbonized to prevent the chemical reaction of the elements with quartz. The quartz ampoule is heated until 723 K (melting point of Te) keeping this temperature for 48 h and shaking all the time using an electromechanical motor. This procedure guarantees the formation of binary species at low temperatures avoiding the existence of free Te at high temperatures, which could produce Te deficiency in the ingot. Then the temperature was slowly increased until 1423 K, with the mechanical shaker always connected for better mixing of the components. After 24 h, the cooling cycle begins until the anneal temperature (800 K) with the mechanical shaker is disconnected. The ampoule is keeping at the annealing temperature for 30 days to assure thermal equilibrium. Then the furnace is switching off, letting naturally cooling the ampoule to room temperature.

2.2 X-Ray Diffraction (XRD)

X-ray powder diffraction data were collected employing a diffractometer (Siemens D5005) equipped with a graphite monochromator (CuK_α $\lambda = 1.54059$ Å) at 40 kV and 20 mA. Silicon powder was used as an external standard. The samples were scanned from $10 - 100°$ 2θ, with a step size of 0.02° and counting time of 20 s. The Bruker analytical software was used to establish the positions of

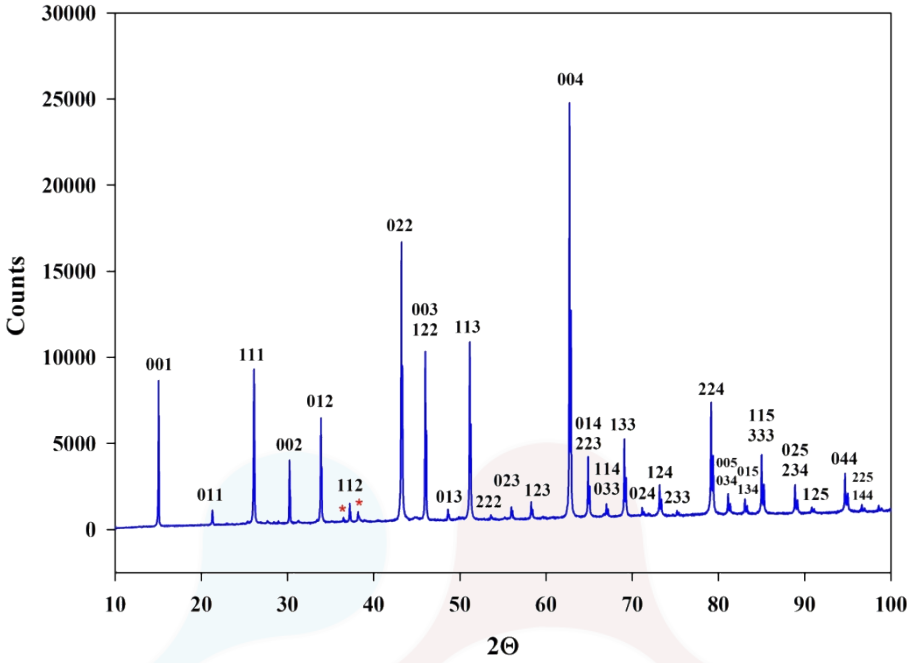

Figure 2: X-ray diffraction pattern of Cu_3TaTe_4. The numbers over the peaks correspond to the hkl-Miller indices. Red asterisks signal two unidentified peaks

the peaks from the CuKα_1 component and to strip mathematically the CuKα2 components from each reflection. The peak positions were extracted employing a single-peak profile fitting carried out through the Bruker DIFFRAC^{plus} software. Each reflection was modeled utilizing a pseudo-Voigt function.

2.3 Scanning Electron Microscopy (SEM)

Stoichiometric relations were investigated by scanning electron microscopy (SEM) technique, using Hitachi S2500 equipment. The microchemical composition was found by an energy-dispersive x-ray spectrometer (EDS) coupled with a computer-based multichannel analyzer (MCA, Delta III analysis, and Quantex software, Kevex). For the EDS analysis, K_α lines were used. The accelerating voltage was 15 kV. The samples were tilted 35 degrees. A standardless EDS analysis was made with a relative error of $\pm(5-10)$ % and detection limits of the order of 0.3 wt %, where the k-ratios are based on theoretical standards.

2.4 Diffuse Reflectance Spectroscopy (DRS)

Optical absorbance has been measured in the energy range 0.5 to 6 eV using Diffuse Reflectance Spectroscopy (DRS) technique using a UV-Visible-IR spectrophotometer equipped with a diffuse reflectance accessory (integrating sphere) capable of collecting the reflected flux. The sample was ground in an agate mortar to obtain a fine powder ($< 10\ \mu m$). Barium sulfate (Merck DIN 5033) was used as an internal standard.

3 Results and discussion

3.1 X-ray diffraction

Figure 2 shown the X-ray diffraction pattern. Using DIVOL06 software [21] the lattice parameter has been calculated as $a = 5.9082$ Å in good agreement with previous reports [22]. Traces of a secondary phase, signaled by red asterisks in Figure 2, are also observed; however, this phase cannot be unambiguously identified with the present information.

Table 1: Scanning Electron Microscopy (SEM) results for Cu_3TaTe_4

	Weight Concentration %			Atom Concentration %		
	Cu	Ta	Te	Cu	Ta	Te
Cu_3TaTe_4_pt1	23.35 ± 0.52	10.06 ± 0.25	66.59 ± 0.70	36.83 ± 0.83	10.85 ± 0.26	52.32 ± 0.55
Cu_3TaTe_4_pt2	23.19 ± 0.54	9.90 ± 0.25	66.91 ± 0.72	36.65 ± 0.85	10.70 ± 0.27	52.65 ± 0.57
Cu_3TaTe_4_pt3	24.31 ± 0.56	8.94 ± 0.23	66.76 ± 0.72	38.18 ± 0.88	9.60 ± 0.25	52.22 ± 0.57
Cu_3TaTe_4_pt4	23.48 ± 0.56	9.69 ± 0.17	66.83 ± 0.73	37.04 ± 0.88	10.45 ± 0.18	52.51 ± 0.58
Cu_3TaTe_4_pt5	23.05 ± 0.56	8.98 ± 0.16	67.97± 0.74	36.56 ± 0.88	9.75 ± 0.18	53.69 ± 0.58
Mean values	23.48	9.51	67.01	37.05	10.27	52.68

3.2 Scanning Electron Microscopy (SEM)

To verify the stoichiometry SEM measurements were performed. Figure 3 display the corresponding microphotography, indicating the five (5) points where the experimental stoichiometry was measured. Table 1 present the obtained values. The calculated nominal stoichiometry of Cu_3TaTe_4, in atom concentration, is Cu = 37.5 %, Ta = 12.5 %, and Te = 50.0 %; the porcentual deviations with respect to the mean experimental values are Cu = 1.2 %, Ta = 17.8 % and Te = 5.4 %.

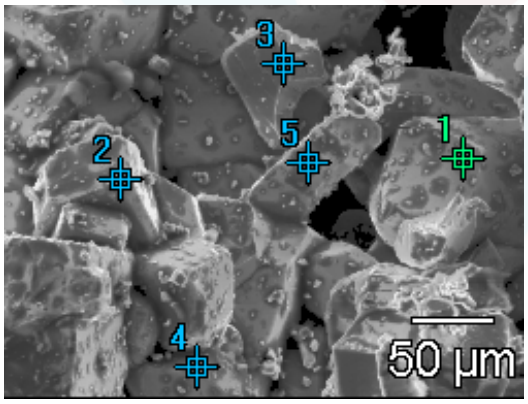

Figure 3: Microphotography of Cu_3TaTe_4. The numbers signal the points where the stoichiometry was measured in correspondence with Table 1

3.3 Diffuse reflectance

The optical absorption of Cu_3TaTe_4 was measured at ambient conditions using the diffuse reflectance technique [23] where the reflectance $F(R_\infty)$ is given by the Equation (1)

$$\frac{K}{S} = \frac{(1-R_\infty)^2}{2R_\infty} = F(R_\infty), \qquad (1)$$

K and S are the absorption and scattering coefficients of the sample, respectively; R_∞ is the reflectance, and $F(R_\infty)$ is usually termed the remission or Kubelka-Munk (K-M) function. Figure 4 show the (K-M) function for Cu_3TaTe_4.

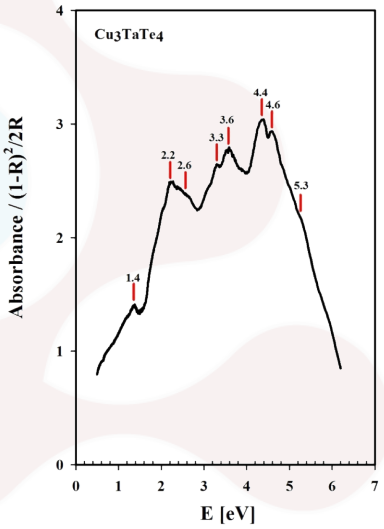

Figure 4: Experimental absorbance for Cu_3TaTe_4. The numbers correspond to the energies of the absorption bands

The experimental absorbance of Cu_3TaTe_4 in the energy interval $1 < E(eV) < 6$ shows several structures or energy bands that, in the absence of other experimental results, can be compared with calculations of Kehoe *et al.* [2], Ali *et al.* [7] and Espinoza *et al.* [8]. It is founding a relatively good agreement because the off-stoichiometric character of real samples is not properly represented in theoretical studies. It was postulated that intrinsic defects within the material affect the bandgap as measured by optical spectroscopy, something

that can be accounted for if excitonic effects were considered [1].

Concerning the energy gap, it is accepted that fundamental band gaps of all sulvanites are naturally indirect [9] because the conduction band minimum (CBM) is located at X point of the Brillouin Zone (BZ) while the valence band maximum (VBM) is located at R point of the BZ [7]. In consequence, indirect transitions are $R \rightarrow X$ type, whereas direct transitions (if they are not forbidden) are at X point.

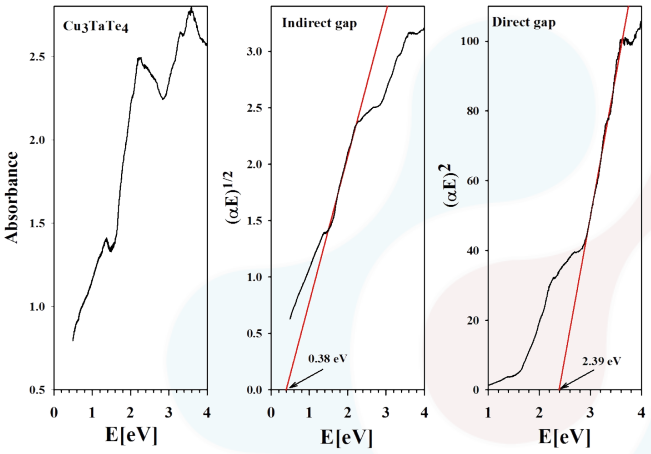

Figure 5: Absorbance (left), indirect (center), and direct (right) optical energy gaps of Cu_3TaTe_4

In Figure 5, using the absorption of Figure 4 and Tauc's plot method [24], direct (X) and indirect ($R \rightarrow X$) transitions values have been obtained founding $E_g^i = 0.38$ eV and $E_g^d = 2.39$ eV. The E_g^i results too much lower than those calculated theoretically. Usually, theoretical calculations produce values that are lower than experimental [7] in consequence the disagreement must become from the polycrystalline character of the sample. The fingerprint of cationic disorder is the broad shoulder in the direct gap curve of Figure 5. Defect states and phonon absorption produce an additional optical absorption at energies a little lower than the bandgap.

The direct gap E_g^d value is higher than those calculated as usually happens. However, the curve of E_g^d fits very well with Tauc's method clearly showing an absorption front. The bandgap of sulvanites increases with the atomic number of the chalcogen atom (S, Se, Te); and effectively, comparing the direct bandgap of Cu_3TaTe_4 (2.39 eV) (this work), Cu_3TaSe_4 (2.43 eV) [22], and Cu_3TaSe_4 (2.76 eV) [25], value of the present work accomplished the empirical rule.

Table 2: Comparative bandgaps values for Cu_3TaTe_4

E_g^i [eV]	E_g^d [eV]	Reference
1.11	1.69	Kahoe *et al.* [2]
1.112, 1.837, 0.972		Ali *et al.* [7]
1.171, 1.323		Hong *et al.* [13]
0.38	2.39	This work

In Table 2, the experimental values are compared with previous calculations.

4 Conclusion

Cu_3TaTe_4 has been synthesized by the melt-anneal method and characterized by DRX, SEM, and Diffuse Absorption. DRX and SEM show a polycrystalline sample with $a = 5.9082$ Å in agreement with previous reports and a stoichiometric deficit of Ta (17.8 %). The indirect and direct bandgaps were measured as $E_g^i = 0.38$ eV and $E_g^i = 2.39$ eV, respectively. These results confirm that Cu_3TaTe_4 may be a good candidate as p-type absorber material for thin-film solar cells with the advantages that their elements are not so toxic as Cd, less expensive than Ga, and more abundant than the rare In, materials that are extensively used in the actuality. Also, it can be used with window materials, as CdS with a lattice mismatch of only 1.53 %.

References

[1] R. Prado-Rivera, C.-Y. Chang, M. Liu, C.-Y. Lai, and D.R. Radu. Sulvanites: The Promise at the Nanoscale. *Nanomaterials*, 11:823, 2021. https://doi.org/10.3390/nano11030823.

[2] A. B. Kehoe, D. O. Scanlon, and G. W. Watson. The Electronic Structure of Sulvanite Structured Semiconductors Cu_3MCh_4 (M = V, Nb, Ta; Ch = S, Se, Te): Prospects

for Optoelectronic Applications. *Journal of Materials Chemistry C3*, C3(12236), 2015. https://doi.org/10.1039/c5tc02760h.

[3] M. A. Ali, N. Jahan, and A. K. M. A. Islam. Sulvanite Compounds Cu_3TMS_4 (TM = V, Nb, and Ta): Elastic, Electronic, Optical, and Thermal Properties using First-principles Method. *Journal Science Research*, 6(3):407–419, 2014. http://dx.doi.org/10.3329/jsr.v6i3.19191.

[4] W.F. Espinosa-García, C.M.Ruiz-Tobón, and J.M.Osorio-Guillén. The Elastic and Bonding Properties of the Sulvanite Compounds: A Girst-principles Study by Local and Semi-local Functionals. *Physica B: Condensed Matter*, 406(20):3788–3793, 2011. https://doi.org/10.1016/j.physb.2011.06.060.

[5] J.M. Osorio-G. and W.F. Espinosa-G. A First-principles Study of the Electronic Structure of the Sulvanite Compounds. *Physica B: Condensed Matter*, 407(6):985–991, 2012. https://doi.org/10.1016/j.physb.2011.12.126.

[6] P. Linus and H. Ralph. The Crystal Structure of Sulvanite, Cu_3VS_4. *Zeitschrift für Kristallographie – Crystalline Materials*, 84(1–6):204–212, 1993. https://doi.org/10.1524/zkri.1933.84.1.204.

[7] M.A. Ali, M. Roknuzzaman, M.T. Nasir, A.K.M.A. Islam, and S.H. Naqib. Structural, Elastic, Electronic, and Optical Properties of Cu_3MTe_4 (M= Nb, Ta) Sulvanites, an Ab Initio Study. *International Journal Modern Physics B*, 1650089, 2016. https://doi.org/10.1142/S0217979216500892.

[8] W.F. Espinosa-G. and S. Pérez-W. and J.M. Osorio-G. and C Moyses A. The Electronic and Optical Properties of the Sulvanite Compounds: A Many-body Perturbation and Time-dependent Density Functional Theory Study. *Journal Physics: Condensed Matter*, 30:035502, 2018. https://doi.org/10.1088/1361-648X/aa9deb.

[9] A.B. Kehoe and D.O. Scanlon and G.W. Watson. Modelling Potential Photovoltaic Absorbers Cu_3MCh_4 (M = V, Nb, Ta; Ch = S, Se, Te) Using Density Functional. *Journal Physics: Condensed Matter*, 28:175801, 2016. https://doi.org/10.1088/0953-8984/28/17/175801.

[10] X.-P. Liu, Z.-Z. Feng, S.-P. Guo, Y. Xia, and Y. Zhang. Promising Thermoelectric Materials of Cu_3VX_4 (X = S, Se, Te): A Cu-V-X Framework Plus Void Tunnels. *International Journal of Modern Physics C*, 30(8):1950045, 2019. https://doi.org/10.1142/S0129183119500451.

[11] J. Peralta and C. Valencia-B. Vibrational Properties of Cu_3XY_4 Sulvanites (X = Nb, Ta, and V; and Y = S, and Se) by Ab initio Molecular Dynamics. *European Physic Journal B*, 90(117), 2017. https://doi.org/10.1140/epjb/e2017-80050-7.

[12] K. Bougherara, F. Litimein, R. Khenata, E. Uçgun, H.Y. Ocak, S. Uğur, G. Uğur, A.H. Reshak, F. Soyalp, and S.B Omran. Structural, Elastic, Electronic, and Optical Properties of Cu_3TMSe_4 (TM = V, Nb, and Ta) Sulvanite Compounds via First-Principles Calculations. *Science of Advanced Materials*, 5(1):97–106, 2019. https://doi.org/10.1166/sam.2013.1435.

[13] A.J. Hong and C.L. Yuan and G. Gu and J. M. Liu. Novel *p*-type Thermoelectric Materials Cu_3MCh_4 (M = V, Nb, Ta; Ch = Se, Te): High Band-degeneracy. *Journal Materials Chemistry A*, 5:9785–9792, 2017. https://doi.org/10.1039/C7TA02178J.

[14] J. Li, H.-Y. Guo, D.M. Proserpio, and A. Sironi. Exploring Tellurides: Synthesis and Characterization of New Binary, Ternary, and Quaternary Compounds. *Journal of Solid State Chemistry*, 117(2):247–255, 1995. https://doi.org/10.1006/jssc.1995.1270.

[15] Y. Liu, M. Liu, and M.T. Swihart. Plasmonic Copper Sulfide-Based Materials: A Brief Introduction to Their Synthesis, Doping, Alloying, and Applications. *Journal Physics Chemistry C*, 121(25):13435–13447, 2017. https://doi.org/10.1021/acs.jpcc.7b00894.

[16] Y. Li, M. Wu, T. Zhang, X. Qi, G. Ming, G. Wang, X. Quan, and D. Yang. Natural Sulvanite Cu_3MX_4 (M = Nb, Ta; X = S, Se): Promising Visible-light Photocatalysts for Water Splitting. *Computational Materials Science*, 165:137–143, 2019. https://doi.org/10.1016/j.commatsci.2019.04.042.

[17] W.F. Espinosa-G., C. Valencia-B., and J.M. Osorio-G. Phononic and thermodynamic properties of the sulvanite compounds: A first-principles study. *Computational Materials Science*, 113:275–279, 2016. https://doi.org/10.1016/j.commatsci.2015.10.036.

[18] F. Hulliger. New semiconductor compounds of the sulvanite type. *Helvetica Physics Acta*, 34:379–382, 1961.

[19] K. Zitter, J. Schmand, K. Wagner, and R. Schöllhorn. Isomer shifts of the 6.2 keV nuclear transition of Ta-181 in sulvanite type ternary phases Cu_3TaX_4 (X = S, Se, Te). *Material Research Bulletin*, 19:801–805, 1984. https://doi.org/10.1016/0025-5408(84)90038-2.

[20] J. Li, H.-Y. Guo, D.M. Proserpio, and A. Sironi. Exploring Tellurides: Synthesis and Characterization of New Binary, Ternary, and Quaternary Compounds. *Journal Solid State Chemistry*, 117:247–255, 1995. https://doi.org/10.1006/jssc.1995.1270.

[21] A Boultif and D. Louer. Powder Pattern Indexing with the Dichotomy Method. *Journal of Applied Crystallography*, 37:724–731, 2004. https://doi.org/10.1107/S0021889804014876.

[22] P. Grima-G., M. Salas, O. Contreras, Ch. Power, M. Quintero, H. Cabrera, I. Zumeta-D., A. Rodríguez, J.A. Aitken, and W. Brämer-E. Cu_3TaSe_4 and Cu_3NbSe_4: X-ray Diffraction, Differential Thermal Analysis, Optical Absorption, and Raman Scattering. *Journal of Alloys and Compounds*, 658:749–756, 2016. https://doi.org/10.1016/j.jallcom.2015.10.283.

[23] P. Kubelka. New Contributions to the Optics of Intensely Light-Scattering Materials. Part I. *Journal of the Optical Society of America*, 38(5):448–457, 1948. https://doi.org/10.1364/JOSA.38.000448.

[24] J. Tauc. Optical Properties and Electronic Structure of Amorphous Ge and Si. *Materials Research Bulletin*, 3:37, 1968. https://doi.org/10.1016/0025-5408(68)90023-8.

[25] P.F. Newhouse, P.A. Hersh, A. Zakutayev, A. Richard, H.A.S. Platt, D.A. Keszler, and J. Tate. Thin-film Preparation and Characterization of Wide Bandgap Cu_3TaQ_4 (Q = S or Se) *p*-type Semiconductors. *Thin Solid Films*, 517:2473–2476, 2009. https://doi.org/10.1016/j.tsf.2008.11.020.